

Analyzing Myocardial Strain using Speckle Tracing from Echocardiograms

Christopher Shen

December 18<sup>th</sup>, 2019

## Abstract

Echocardiography is a non-invasive diagnostic tool that can be used to evaluate cardiac myocardium function. Strain and strain rate imaging have recently emerged as critical tools to estimate myocardial function. Traditionally, this method would require Doppler imaging in order to determine the velocity of the tissue, which can later be used to determine strain and strain rate. Recently, non-Doppler strain imaging has emerged as a promising technique that could overcome the limitations of Doppler imaging. This new method labels and tracks clusters of pixels that encompass speckle in the ultrasonic image. Even more recently, the segmentation of the cardiac tissue may no longer be needed and can be replaced by pixel-by-pixel tracking. In this report we show the validity of tracking every pixel in an echocardiogram. By doing so, valuable myocardium characteristics can be determined. This can in turn be used as a diagnostic tool for rapid and accurate assessment of many subclinical applications.

## Introduction

Chest pain is the second most common complaint in emergency departments in the United states, accounting for approximately 7.6 million visits a year<sup>2</sup>. Due to the emergent nature of these cases, echocardiograms serve as an essential tool not only for ruling out aortic dissections, but also for evaluating ventricular function and the presence of regional wall motion abnormalities<sup>3</sup>. There are other modalities that are used to assess causes of chest pain, such as X-Rays, ECGs, and cardiac enzyme level tests, but these methods are often resource expensive. Because of these limitations, echocardiography is now deemed as an important imaging technique for the assessment of left ventricular systolic and diastolic function, among other myocardial functions<sup>3</sup>.

Traditionally, myocardial function has been assessed with echocardiography by visual estimation of wall motion<sup>4</sup>. Left ventricular function can be determined by estimating end-diastolic and end-systolic volumes, which generally requires the accurate detection of endocardial borders<sup>5</sup>. Once the edges of the borders have been determined, a modified Simpson rule can be used to calculate the volume of the left ventricular cavity. This is done by simplifying the geometry of the left ventricle and using a few measurements determined visually to calculate disk slices, which are subsequently summed. Thickening of the myocardial wall and movement of the endocardium requires the segmentation of wall motion<sup>4</sup>. However, the qualitative approach of determining segmentation, wall thickness, and wall motion all require expert knowledge and are prone to intra-observer and inter-observer variability<sup>6</sup>. Not only this, but this qualitative method has limited capability of evaluation radial displacement and deformation and determine myocardial twisting<sup>7</sup>. These sources of variability make the identification of subtle abnormalities difficult and as a result may lead to therapeutic implications.

In the late 1990s, strain rate was proposed as a quantitative method for analyzing echocardiograms for ventricular function<sup>8</sup>. Perk et al. showed that strain is defined as a dimensionless parameter that represents the deformation of an object of interest. It is expressed as a fractional change from the original dimensions of the object of interest and is defined as:

$$S = \frac{\Delta L}{L_0} = \frac{L - L_0}{L_0} \quad (1)$$

where  $S$  is the longitudinal strain,  $\Delta L$  is the change in length, and  $L_0$  is the original length of the object. Strain rate is defined as the change of strain with respect to time or taking the time derivative of Equation (1).

$$SR = \frac{S}{\Delta t} = \frac{\Delta L/L_0}{\Delta t} = \frac{\Delta L/\Delta t}{L_0} = \frac{V}{L_0} \quad (2)$$

where  $SR$  is the strain rate and  $V$  is the velocity of the segmented tissue<sup>4</sup>. We can see that strain rate can be determined using Doppler imaging since Doppler can elucidate the velocity of tissues moving. Once the strain rate is obtained, we can integrate the value to gain the strain of a particular tissue segment as strain rate is the first-order time derivative of strain. It has been shown that strain and strain rate can be used as faithful quantitative tools for determining ventricular function that is less prone to subjective human interpretation<sup>9</sup>. Traditionally, Doppler imaging with subsequent strain analysis can be used to diagnose many diseases such as cardiomyopathy, cardiac dyssynchrony, ventricular, and arterial functions<sup>10</sup>. However, there are also limitations to this technique as this derivation is dependent on Doppler imaging, which is angle dependent, which leads to the topic of this report. Instead of depending on Doppler imaging, this report determines the pixel-by-pixel deformation in a two-dimensional echocardiogram.

Non-Doppler two-dimensional imaging is a newer technique that was first proposed in 2007 and, on a high level, analyzes the motion of tissue by tracking speckles in the ultrasonic image<sup>4</sup>. The technique proposed by Perk et al. suggests labeling large speckles, roughly twenty to forty pixels in diameter, and tracking the labeled groups frame by frame. By doing so, the velocity of the tissue can be determined as the acquisition frame rate is known. In this report, instead of labeling groupings of pixels, we are instead interested in labeling every single pixel in an ultrasonic image. By doing so, there would not be a need to segment the image and would be less prone to the subjective nature of human analysis. In this report, we show an algorithmic method to track individual pixels in consecutive frames. The deformation of the cardiac tissue can then be extrapolated and can be used further downstream to determine strain and strain rate.

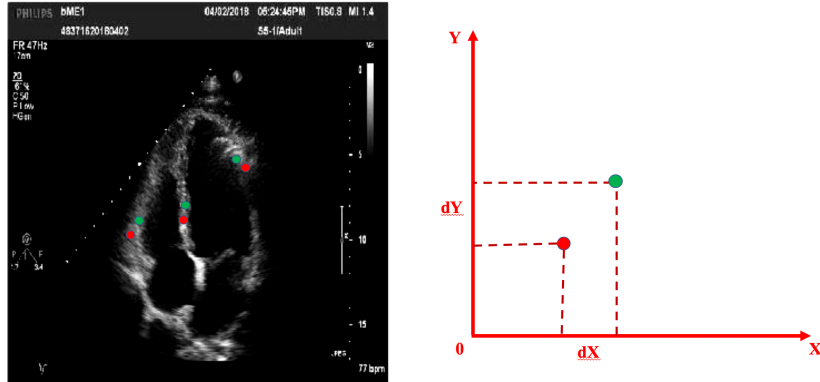


**Figure 1** The red dots on the image represent the original coordinate location of an individual pixel and the green dots represent the coordinate location on the next frame of the movie. The two-dimensional deformation vector is calculated, dX and dY. Figure adapted from American Society of Echocardiography<sup>11</sup>

## Methods

To begin this procedure, two-dimensional B-mode ultrasonic echocardiograms are obtained. The videos are imported into Matlab and are transformed into a grayscale movie stack. The movie stack is transformed into a three-dimensional matrix where the dimensions of the x and y axes are the width and height of the image, respectively. The z-axis of the three-dimensional matrix is the time axis. The values stored in these arrays are 8-bit values ranging from 0 to 254 where 0 represents a completely black pixel and 254 represents a completely white pixel. All of the videos that were obtained were between 49 frames and 54 frames, so the z-axis length ranged from 49 to 54. All of the videos were acquired at 47 frames per second. All of these characteristics were determined using Matlab video processing libraries and all variables were temporarily stored. The millimeter per pixel value was manually calculated using the scale present on the ultrasonic image and is stored as well.

Once the video is loaded into an 8-bit three-dimensional matrix, the movement of the tissue is determined. The general principle behind this calculation is that the tissue in ultrasonic images is represented with white pixels. As the tissue contracts, the overall number of pixels that are white in the frame will be reduced since the tissue is physically getting smaller during systole. This means that the difference in total number of bright pixels between the systole frame and the diastole frame will be non-zero. Thus, movement of the tissue is indirectly determined by reducing each two-dimensional frame into a one-dimensional value, which represents the difference in total pixel brightness within each frame when compared to a user determined baseline frame. Each value is then plotted frame-by-frame to produce a two-dimensional trace, which indirectly represents the movement within the movie. Determining the movement trace is useful as it will enable us to create a mask later on and will allow the user to quantitatively determine when the diastole frame occurs (Figure 2).

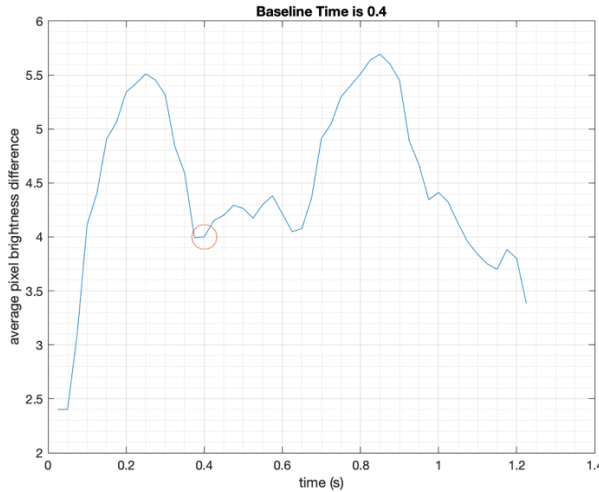


**Figure 2** A representative movement trace from a four-chamber apical view echocardiogram with the red circle highlighting the frame chosen as the baseline or end-diastole frame

The baseline, or end-diastole frame, is determined from the movement trace. This frame will be used to calculate the frame-by-frame pixel-by-pixel deformation using an external Matlab library. The library labels each pixel and determines the similarity of the labeled pixel to the pixels of a consecutive frame. The similarities are stored and once each original pixel has been paired with a pixel in the next frame the forward transform is calculated. The transform is stored as a vector, which represents where each pixel has moved with respect to the previous frame. The matrix of transformation vectors is then saved as this calculation is computationally expensive. This allows us to calculate deformations as an independent step with analysis not dependent on directly succeeding this step.

Each frame's deformation matrix is then loaded by iterating through every saved matrix. A video mask is generated in order to save computational resources and mapping vectors of non-moving or non-tissue regions would result in extraneous data. The brightness of each pixel of the original movie stack is correlated against the movement trace calculated in the previous step. The idea here is that pixels that are part of the tissue will very closely correlate to the movement trace and pixels that are outside of the region of interest will not correlate closely to the movement trace. This will then produce a video mask that can be used to save resources and produce a cleaner overlay (Figure 3).

Once a video mask is produced the deformation vectors that are outside of the mask are deleted as they do not contain relevant data. Then the average deformation per frame is calculated by simply calculating the average of all the deformation vectors. This value is stored as it will be useful to show that the movement of the tissue can also be represented by the average deformation in each frame. An overlay of vectors is generated using an external Matlab library called quivercolorbar. This library allows us to input a baseline deformation vector frame and the transformed deformation vector frame and it will map a vector with a varying color intensity to represent the deformation of the pixels. The original baseline frame is shown, with the colored vectors overlaid,

and the moving frame is also overlaid on the original frame. This will create a video of the moving cardiac tissue with vectors showing the deformation of the pixels.

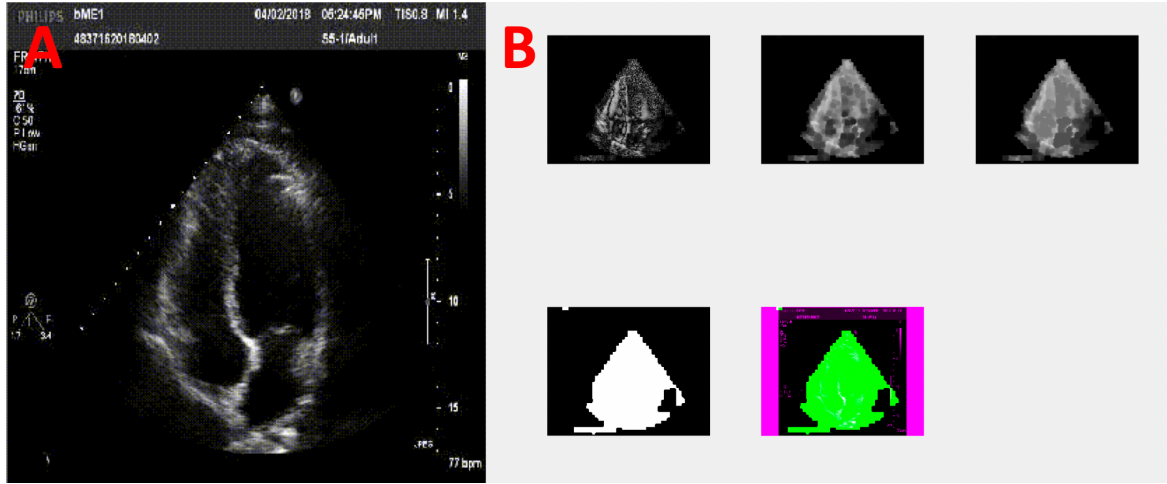


**Figure 3** (A) Original B-mode frame (B) Video mask that is produced by calculating the correlation of each pixel through time against the movement trace, where un-correlated pixels are not included in the video mask. The mask is filled in by expanding points of interest with disks.

A validation test was conducted in order to ensure the validity of this method. To do this, a circle is generated with the radius of the circle slowly growing and shrinking. The rate and magnitude of the change in radius is determined and noted as it will subsequently be compared to the values produced by the algorithm outlined above. The goal of the validation test is to ensure that the tracking of pixel-by-pixel movement is correct when compared to a known value.

## Results

Three set of experiments were conducted for this report. Four-chamber apical view, mitral valve view, and papillary valve view echocardiograms were analyzed using the aforementioned method. Figure 4 shows the key frames from the mitral valve view and the analysis of those frames overlaid on top of the original image.

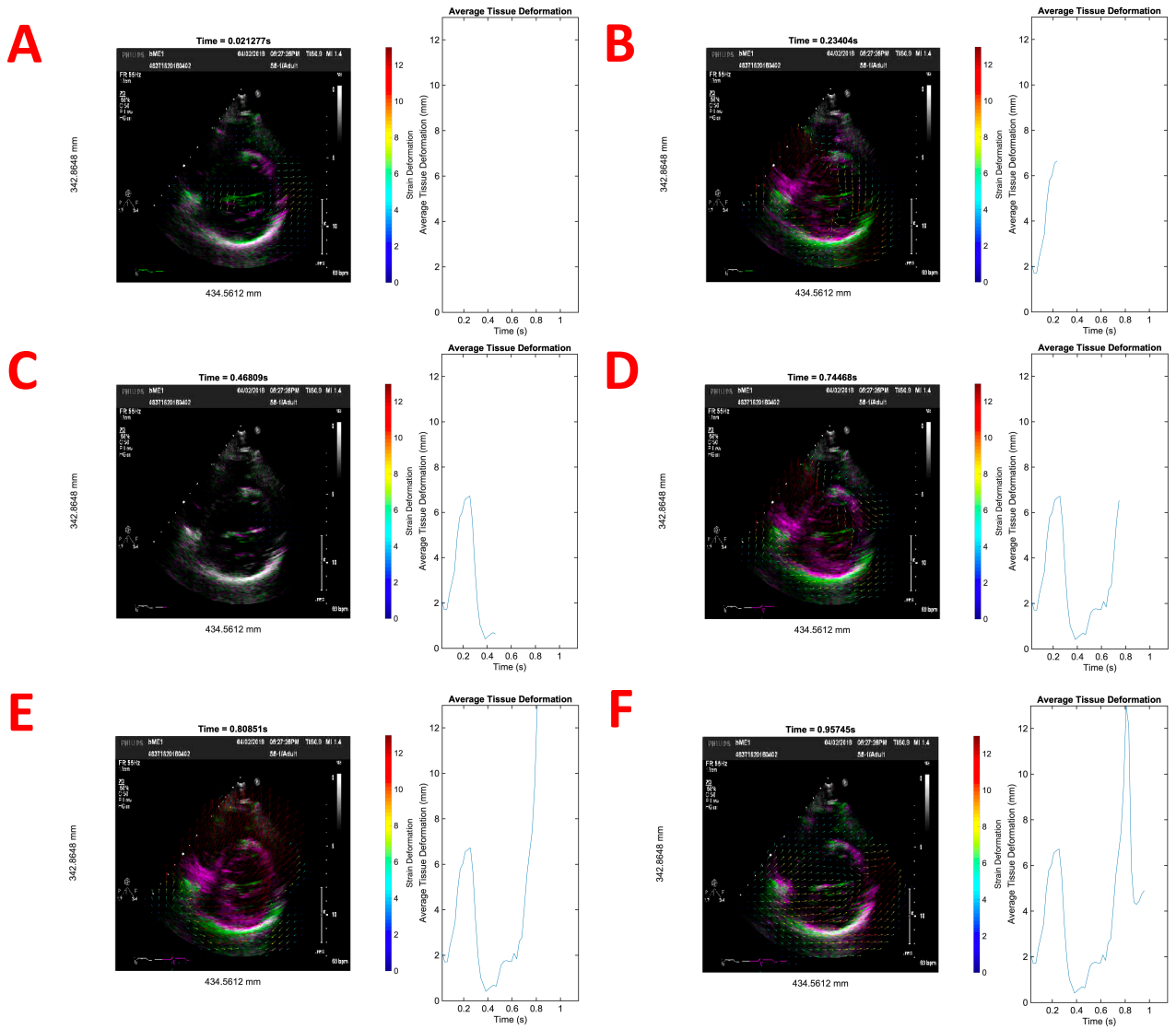


**Figure 4** (A-F) Represent six different time-points in a mitral valve view echocardiogram. Each pane has the original image represented in green with the moving frame represented in purple. The colored vectors represent the magnitude of the deformation along with the direction of the deformation. The graph on the right side of each pane represents the average deformation throughout the entire frame and closely aligns with the movement of the frame.

We see that the analysis of deformation closely aligns with what we expect physiologically. Even though this is a two-dimensional image, we can see that the valve is closing towards the center of the valve with the tissue collapsing towards the center. The mitral valve is calculated to have approximately 7-8mm of deformation. The relative magnitudes of the vectors are correlated to physiological levels.

Figure 5 shows key frames from the papillary valve view and the analysis of those frames overlaid on top of the original image.

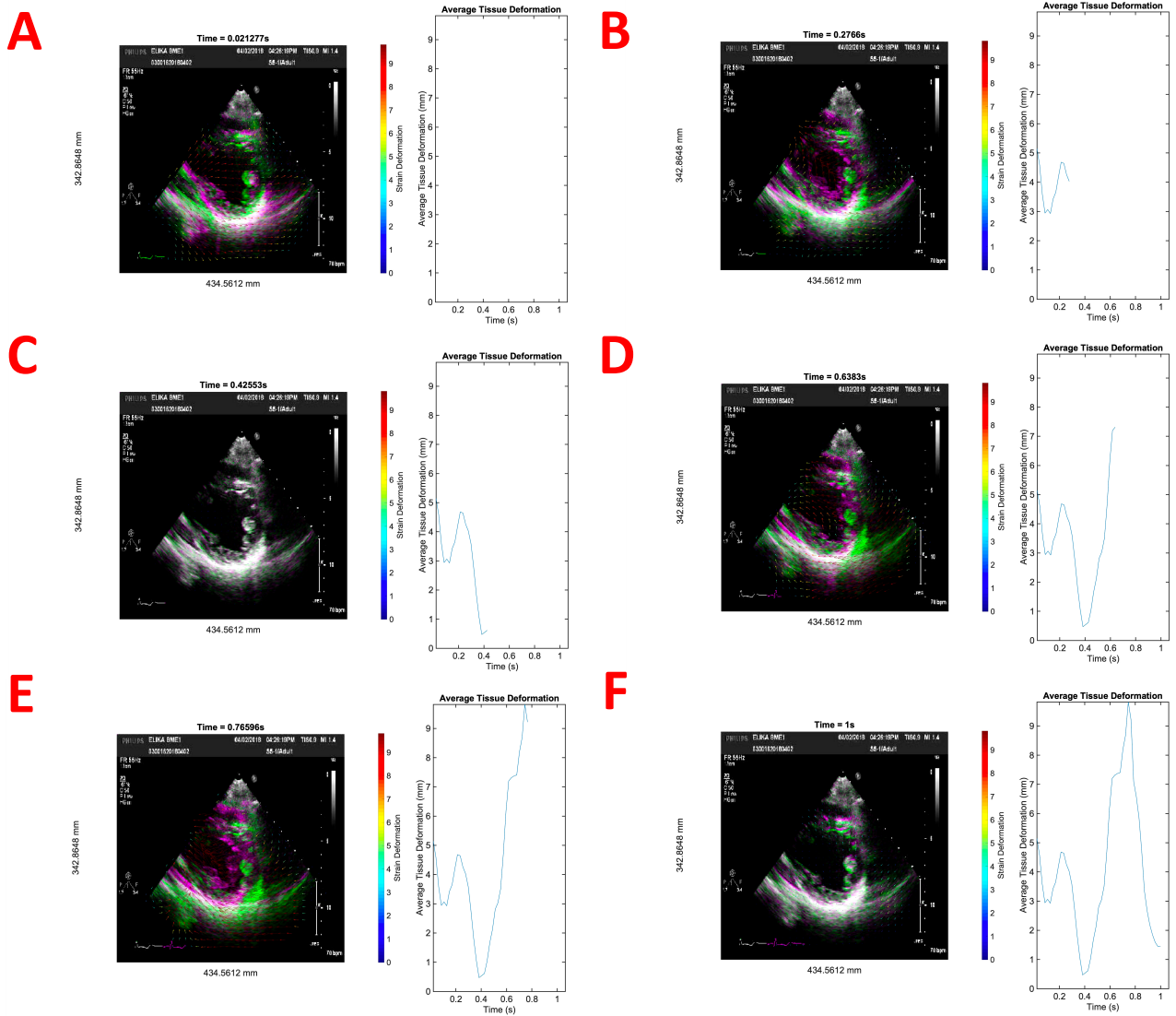


**Figure 5 (A-F)** Represent six different time-points in a papillary valve view echocardiogram. Each pane has the original image represented in green with the moving frame represented in purple. The colored vectors represent the magnitude of the deformation along with the direction of the deformation. The graph on the right side of each pane represents the average deformation throughout the entire frame and closely aligns with the movement of the frame.

We also see that the analysis of the deformation of the papillary valve closely aligns with what we expect physiologically. We can see that the valve is closing towards the center of the valve with the tissue collapsing towards the center. We see that the average deformation when the papillary valve closes is approximately 6mm with the relative magnitudes of the vectors correlating to physiological levels.

Finally, Figure 6 shows six frames from the four-chamber apical view and the analysis of the frames are overlaid over the original frame.

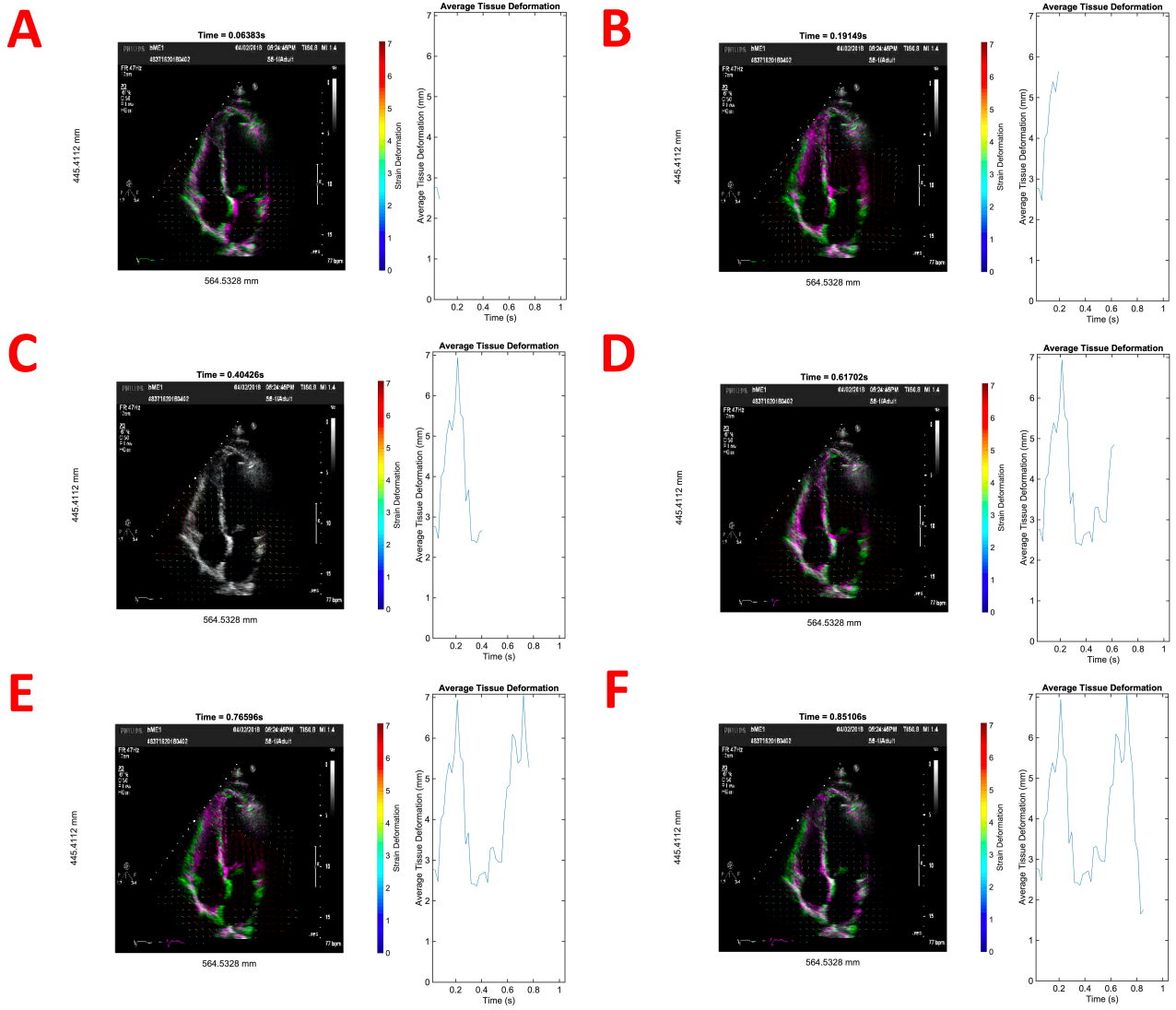


**Figure 6 (A-F)** Represent six different time points in a four-chamber apical view echocardiogram. Each pane has the original image represented in green with the moving frame represented in purple. The colored vectors represent the magnitude of the deformation along with the direction of the deformation. The graph on the right side of each pane represents the average deformation throughout the entire frame and closely aligns with the movement of the frame.

We see in Figure 6 that the deformation of the cardiac myocardium propagates from the top of the heart down towards the apex of the heart. The magnitude and the direction of the deformation vectors align with what is expected physiologically with the average tissue deformation of approximately 7mm aligning closely with previously published values<sup>12</sup>.

Validation of this method was conducted on a movie of a circle growing and shrinking. The rate and magnitude of change is pre-determined. The radius of the circle increases or decreases by one unit per frame with each radius unit equivalent to 3 pixels in the movie. The radius of the circle increases by a total of 20 units before shrinking back to the original dimensions. Figure 7 shows the deformation of the known circle along with the average deformation of the circle.

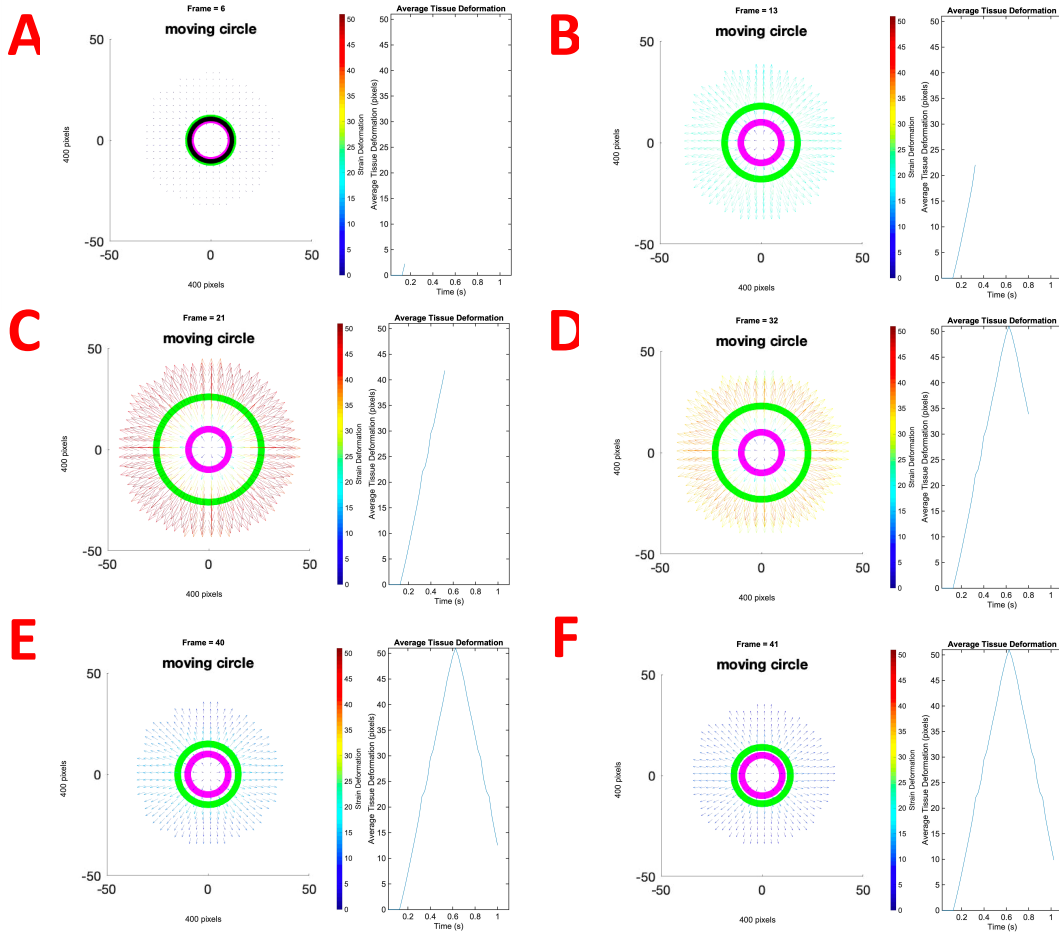


**Figure 7 (A-F)** Represent the deformation of a generated circle that is growing and shrinking at a known rate. The first frame with movement is frame 6 and at frame 25 is the maximal deformation.

The validation using the predetermined growing and shrinking circle validates our deformation analysis. The validation video has 6 frames at the beginning with no movement in order to allow for accurate determining of baseline frame. There is a total of 44 frames in the video with the last frame mirroring the original dimension of the circle. At frame 21 there is 15 frames of movement with each frame representing 3 pixels. We see that at frame 21 there is approximately 43 pixels of deformation. Furthermore, at frame 40, with only 4 frames left until the end of the shrinking circle, there is approximately 13 pixels of deformation. This makes sense as there are 4 frames for the

circle to return to 0 deformation and since each frame represents 3 pixels of deformation it works out.

## Discussion

In this report we have shown a method to determine the deformation of an echocardiographic video without the need of human segmentation or Doppler imaging. The method relies on the identification and tracking of individual pixels in an ultrasonic image. The method is validated through the analysis of a movie with known deformation. The deformation values for both the mitral and papillary valves were significantly different than published values. In our report, we calculated of 7-8mm for the mitral valve and 6mm for the papillary valve. This is significantly different than a reported value of 2mm for mitral valve deformation<sup>13</sup>. Our reported value of 6mm for papillary valve is also significantly different than published values of approximately 2mm as well<sup>14</sup>.

Sources of error for these calculations may help us determine the reason for these differences. One major area to note is the dimensions of both valves according to the analysis. Previously reported diameters for the mitral annulus are around 3.15cm whereas the approximate diameter according to our analysis has the mitral annulus at approximately 10cm. Furthermore, the papillary valve for both the reported value and the calculated values in this report also differ where reported values are approximately 3cm and analyzed values of approximately 10cm<sup>1</sup>. This error could be attributed to the invalid scaling factor of mm per pixel. We can see that if the dimensions of the valves are scaled down one-third to what has been previously reported, the deformation would also be roughly 2mm for both the mitral and papillary valves.

We show in this report that the average deformation in the four-chamber apical view to be approximately 7mm at the end-systole frame. This in fact does align closely with published values where three-dimensional ultrasonic analysis has shown physiological deformation to be approximately 6-8mm depending on where the measurement is taken<sup>12</sup>. The reason why the four-chamber view was closer to physiological levels may be attributed to a more accurate determination of scaling ratio.

The directions and relative magnitudes of the vectors are physiologically correct but there are many extraneous vectors that are both within the cavity of the ventricles or outside of the cardiac myocardium. The existence of these vectors could be more carefully removed by applying a more intelligent automatic video mask generator. The current method of correlating the change of brightness for every pixel with respect to the overall movement trace generates a lot of false positive values for the video mask. These extra values should be removed in order to make the average deformation value more correct as the amount of noise would be reduced when these extra vectors are removed.

## Conclusion

We have shown that non-doppler two-dimensional echocardiography can be analyzed to provide rapid and accurate assessment of cardiac myocardium elastography. The only input for the algorithm outlined above is a post-processed two-dimensional B-mode echocardiogram. The output of the analysis provides real-time deformation overlaid on the original video. In the report we show that the values obtained from the analysis can be physiologically close and with some more fine tuning the analysis could produce physiologically accurate results. The analysis provides for an observer-independent analysis that does not rely on Doppler imaging. Not only this, the analysis provides for a quantitative assessment that is reproducible. The output is a video that can be easily interpreted by non-expert observers and can show subtle differences in the properties of the cardiac myocardium.

This kind of analysis can provide for rapid diagnosis of many cardiovascular implications. One potential application can be detecting cardiac dyssynchrony. Cardiac dyssynchrony occurs when peak longitudinal, axial, or radial strains are not reached at the same time point across the cardiac myocardium. This misalignment would be difficult to detect with only subjective and observer-based analysis. The visualization of tissue deformation could showcase the subtle differences of when peak strain is reached.

Not only that, the detection of late subclinical consequences of cancer therapies is also a very useful application of this sort of technology. If a chemotherapy is completed, patients are often observed for a period of time afterwards to check on cardiotoxicity as many chemotherapies are toxic to cardiac muscles. However, cardiotoxicity may present several years after therapy<sup>15</sup>. This has led to an increase interest in detecting subclinical cardiotoxicity in cancer survivors using myocardial deformation parameters<sup>16</sup>. Ultrasound provides for a non-invasive diagnostic tool that when coupled with this kind of analysis could show myocardial deformation abnormalities. Overall, these are just two applications for this technology and there are many more that have not been gone over.

## Future Work

The analysis conducted in this report is computationally expensive as every pixel is labeled and tracked throughout the ultrasonic image. Each frame takes approximately 2.5 minutes to compute with each video consisting of approximately 50 frames. This leads to a computation time of over two hours per video. Future work may entail partitioning the computational load across many processors and conducting the analysis in parallel. This can be done using distributed arrays and multiple worker pools to allow for maximal utilization of a computer's resources. Some of the computational load can be processed much faster if the work was computed on the cloud, as cloud resources will nearly always supersede the resources of a personal cluster.

Finally, this report only handled healthy cardiac myocardium. Future work could entail comparing and classifying diseased patients and determining whether or not this algorithm can correctly identify them. The limitation of testing primarily occurred as acquiring diseased hearts could not

be done. By obtaining echocardiograms of diseased hearts, this algorithm can be verified to show subtle differences in deformation.

### **Acknowledgments**

- Echocardiogram videos were graciously provided by Rachel Weber, Nilofaur Saharkhiz, Jad El Harake
- Thank you to Dr. Konofagou for providing the infrastructure and knowledge to conduct these experiments

## References

1. Dwivedi, G., Mahadevan, G., Jimenez, D., Frenneaux, M. & Steeds, R. P. Reference values for mitral and tricuspid annular dimensions using two-dimensional echocardiography. *Echo Res. Pract.* **1**, 43–50 (2014).
2. Hollander, J. M. C. Evaluation of the adult with chest pain in the emergency department - UpToDate. <https://www.uptodate.com/contents/evaluation-of-the-adult-with-chest-pain-in-the-emergency-department> (2018).
3. Esmaeilzadeh, M., Parsaee, M. & Maleki, M. The role of echocardiography in coronary artery disease and acute myocardial infarction. *Journal of Tehran University Heart Center* vol. 8 1–13 (2013).
4. Perk, G., Tunick, P. A. & Kronzon, I. Non-Doppler Two-dimensional Strain Imaging by Echocardiography-From Technical Considerations to Clinical Applications. *Journal of the American Society of Echocardiography* vol. 20 234–243 (2007).
5. Foley, T. A. *et al.* Measuring left ventricular ejection fraction-techniques and potential pitfalls. *Eur. Cardiol.* **8**, 108–114 (2012).
6. Hoffmann, R. *et al.* Analysis of interinstitutional observer agreement in interpretation of dobutamine stress echocardiograms. *J. Am. Coll. Cardiol.* **27**, 330–336 (1996).
7. Mehrotra, R., Alagesan, R. & Srivastava, S. Quantitative assessment of left ventricular systolic function using 3-dimensional echocardiography. *Indian Heart Journal* vol. 65 620–628 (2013).
8. Sonnenblick, E. H., Parmley, W. W., Urschel, C. W. & Brutsaert, D. L. Ventricular function: Evaluation of myocardial contractility in health and disease. *Prog. Cardiovasc. Dis.* **12**, 449–466 (1970).
9. Hashimoto, I. *et al.* Myocardial Strain Rate Is a Superior Method for Evaluation of Left Ventricular Subendocardial Function Compared with Tissue Doppler Imaging. *J. Am. Coll. Cardiol.* **42**, 1574–1583 (2003).
10. Abraham, T. P., Dimaano, V. L. & Liang, H.-Y. Role of tissue Doppler and strain echocardiography in current clinical practice. *Circulation* **116**, 2597–609 (2007).
11. Leitman, M. *et al.* Two-dimensional strain-A novel software for real-time quantitative echocardiographic assessment of myocardial function. *J. Am. Soc. Echocardiogr.* **17**, 1021–1029 (2004).
12. Moore, C. C., Lugo-Olivieri, C. H., McVeigh, E. R. & Zerhouni, E. A. Three-dimensional systolic strain patterns in the normal human left ventricle: Characterization with tagged MR imaging. *Radiology* **214**, 453–466 (2000).
13. Ben Zekry, S. *et al.* Patient-Specific Quantitation of Mitral Valve Strain by Computer Analysis of Three-Dimensional Echocardiography: A Pilot Study. *Circ. Cardiovasc. Imaging* **9**, (2016).
14. Ayoub, S. *et al.* Heart valve biomechanics and underlying mechanobiology. *Compr. Physiol.* **6**, 1743–1780 (2016).
15. Yeh, E. T. H. & Bickford, C. L. Cardiovascular complications of cancer therapy: incidence, pathogenesis, diagnosis, and management. *Journal of the American College of Cardiology* vol. 53 2231–2247 (2009).
16. Thavendiranathan, P. *et al.* Use of myocardial strain imaging by echocardiography for the early detection of cardiotoxicity in patients during and after cancer chemotherapy: A

systematic review. *Journal of the American College of Cardiology* vol. 63 2751–2768 (2014).